Search for evidence of rotational cluster bands in ^{18}O

S. Pirrie,[1] C. Wheldon,[1] Tz. Kokalova,[1] J. Bishop,[1,*] Th. Faestermann,[2] R. Hertenberger,[3] H.-F. Wirth,[3] S. Bailey,[1] N. Curtis,[1] D. Dell'Aquila,[4,†] D. Mengoni,[5] R. Smith,[1,‡] D. Torresi,[1,§] and A. Turner[1]

[1]*School of Physics and Astronomy, University of Birmingham, Birmingham B15 2TT, United Kingdom*
[2]*Physik Department, Technische Universität München, D-85748 Garching, Germany*
[3]*Fakultät für Physik, Ludwig-Maximilians-Universität München, D-85748 Garching, Germany*
[4]*Dipartimento di Fisica, Università degli Studi di Napoli Fedorico II, 80138 Napoli NA, Italy*
[5]*Dipartimento di Fisica e Astronomia, Università degli Studi di Padova, 35122 Padova PD, Italy*

(Received 24 April 2020; revised 17 June 2020; accepted 26 October 2020; published 14 December 2020)

Clustering in ^{18}O is of great interest to the nuclear physics community, due to theoretical predictions of core+α and nuclear molecular structures. An experiment was performed in order to measure branching ratios for states in ^{18}O, determining the tendency towards clustering based on the value of $\Gamma_\alpha/\Gamma_{\rm tot}$ for each state, and the reduced widths compared to the Wigner limit. An experimental method that enables the measurement of branching ratios for almost all available decay modes, including γ decay, α decay, and n decay, was employed. The method is also sensitive to the population of excited states in daughter nuclei, allowing for more accurate determination of the α_0 branch. The measurements represent, for several states, either the first branching ratio measurement or the first determination of $\Gamma_\alpha/\Gamma_{\rm tot}$. Based on these measurements, no evidence of consistent cluster structure is seen across any of the bands previously proposed, casting doubt on their existence. Despite this, some states displaying cluster structure are observed.

DOI: 10.1103/PhysRevC.102.064315

I. INTRODUCTION

The study of the nuclear force provides a difficult challenge, ultimately requiring the ability to describe and predict all possible nuclear configurations as they appear in nature. The nuclear shell model is one of the most successful models for this purpose, being able to predict both ground and excited state properties for a multitude of nuclei. However, there are many configurations, in particular collective-mode excitations, that the shell model cannot accurately describe or predict. The existence of these collective-mode behaviors provides excellent tests for nuclear models while also allowing for many body problems to be reduced and hence the required computational power decreased.

An important instance of such a phenomenon is the ability for α clusters to form as substructures in nuclei, due in part to the large binding energy per nucleon of the α particle. This phenomenon is well established in light $N = Z$ even-even nuclei [1,2], and is essential for the formation of elements in stars. Common α-cluster configurations in these nuclei involve one or more α particles orbiting a core consisting of the remaining nucleons, such as the extensively studied ^{16}O $\bigotimes \alpha$ system in ^{20}Ne [3,4], or of total dissociation of the nucleus into an $N\alpha$ system, as in the ^{12}C Hoyle state [5]. Extending to neutron-rich systems, configurations involving valence neutrons can be observed with increased stability, due to cores being bound together by the valence neutrons. These neutrons act analogously to electrons binding atoms together in covalent bonds, and hence these systems are known as nuclear molecules [1,2]. There has been much interest in potential cluster structures in ^{18}O, with notable experimental measurements by Avila *et al.* [6], Yang *et al.* [7], Goldberg *et al.* [8], and Johnson *et al.* [9].

An experiment, performed at the Maier-Leibnitz Laboratory in Munich by von Oertzen *et al*. [10], measured excitation functions of ^{18}O for a series of angles. Using the states measured, rotational bands were proposed, with four of them proposed to have cluster structures (the positive-parity and negative-parity signatures of each structure are distinct due to broken intrinsic reflection symmetry): the $K^\pi = 0_2^{+/-}$ with a proposed ^{14}C $\bigotimes$ α structure [11,12] and the $K^\pi = 0_4^{+/-}$ with a proposed 6p-4h structure [13], which might be interpreted as a molecular ^{12}C $\bigotimes$ $2n$ $\bigotimes$ α structure [14]. Additionally, two shell-model bands (the ground-state band and single-proton excitation $K^\pi = 1^-$ band) were also suggested.

In order to determine the validity of these cluster bands, the tendency towards clustering of each state must be determined. This can be done by calculating the reduced partial α width, γ_α^2, of each state in the band through the determination of the

*Present address: Cyclotron Institute, Texas A&M University, College Station, TX 77840, USA.
†Present address: Ruđer Bošković Institute, Bijeni/vc 54, HR-10000 Zagreb, Croatia.
‡Present address: Department of Engineering and Mathematics, Sheffield Hallam University, City Campus, Howard Street, Sheffield S1 1WB, United Kingdom.
§Present address: INFN Laboratori Nazionali del Sud, Via S. Sofia, 62, 95125 Catania CT, Italy.

α-branching ratio. These widths can then be compared to the Wigner limit defined by

$$\gamma_W^2 = \frac{3\hbar^2}{2\mu r^2}, \tag{1}$$

where μ is the reduced mass of the two-body exit channel and r is the channel radius, to determine $\theta_\alpha^2 = \gamma_\alpha^2/\gamma_W^2$ [15].

An experimental method was used in order to extract branching ratios for the high-energy excited states in ^{18}O to allow for determination of $\gamma_\alpha^2/\gamma_W^2$, utilizing high-resolution reconstruction of decay products detected in the Birmingham large-angular-coverage double-sided silicon strip detector (DSSD) array through kinematic techniques [16]. Establishment of the detection efficiency of each decay channel, as well as distinguishing between population of excited levels in daughter nuclei and consequent further decays, was done through Monte Carlo simulation [17–19]. The Monte Carlo data were used to set gates on regions of the experimental data, allowing for the measurement of many different decay channels. In this way, areas of loci that overlapped could also be disentangled. The value of $\Gamma_\alpha/\Gamma_{t\alpha}$ was then extracted by normalizing over the sum of all of the events from measured decay modes after efficiency corrections.

II. EXPERIMENTAL METHOD

To measure the branching ratios in ^{18}O, an experiment was performed at the Maier-Leibnitz Laboratory (MLL). The [^{12}C(^{7}Li, p) ^{18}O*] reaction was utilized using the Q3D magnetic spectrograph [20,21], but additionally, the Birmingham large-angular-coverage DSSD array was placed in the target chamber to enable the high-resolution reconstruction of decay products from ^{18}O, from which the branching ratios were determined. A 44.0 MeV ^{7}Li beam provided by the Van de Graaff Tandem accelerator was incident on a 110 μg/cm^2 natural C target. The recoil proton produced was detected in the Q3D, set in plane at an angle of -39.0° with an angular acceptance of $\pm 3.0^\circ$ in plane and $\pm 2.0^\circ$ out of plane. The overall experimental setup is depicted in Fig. 1.

After deflection by the magnetic elements of the Q3D, charged particles were incident on a focal-plane detector, described in detail in Ref. [22]. This focal-plane detector enabled measurements of energy loss, precise position, and residual energy of the incident particles. Particle-identification techniques were then employed to identify and distinguish protons of appropriate energies, removing background caused by other reaction channels. Due to the ability of the Q3D to correct for the kinematic shift, i.e., the dependence of the ejectile energy on the reaction angle, the position measurement directly provided the excitation energy of the residual nucleus [23] and allowed for the measurement of excitation functions at a range of energies. The focal-plane detector was calibrated by comparison of the known energies of states in ^{18}O and the measured position. The observed excitation regions were $E_x = 7.8$ MeV (range $6.8 \rightarrow 9.4$ MeV); $E_x = 10.5$ MeV (range $9.6 \rightarrow 11.9$ MeV); $E_x = 13.2$ MeV (range $12.4 \rightarrow 14.5$ MeV); and $E_x = 15.1$ MeV (range $14.4 \rightarrow 16.3$ MeV).

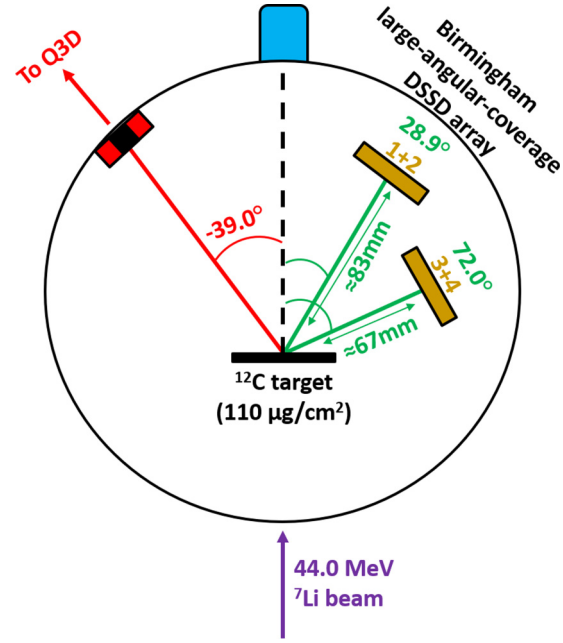

FIG. 1. A representation of the experimental setup used, showing the positions of the Birmingham DSSD array and the Q3D magnetic spectrograph in plane.

In order to determine the species of decay products from ^{18}O*, the Birmingham DSSD array was used in conjunction with the Q3D to enable high-resolution reconstruction of the decay products. The Birmingham DSSD array comprises four 500 μm 50×50 mm^2 W1 (Micron Semiconductor Ltd) [24] DSSDs, the active area of which was segmented into 16 horizontal and 16 vertical strips. The DSSDs were placed in a 2×2 configuration so as to give a total angular coverage of $14^\circ \rightarrow 92^\circ$ in-plane and $-36^\circ \rightarrow 40^\circ$ out of plane, and were calibrated through use of a triple-α source composed of ^{239}Pu, ^{241}Am, and ^{244}Cm.

A. Decay channels

For ^{18}O, several particle-decay channels become energetically allowed within the observed excitation regions. The relevant energy thresholds are $S_\alpha = 6.227$ MeV, $S_n = 8.045$ MeV, $S_{2n} = 12.188$ MeV, $S_{n\alpha} = 14.404$ MeV, and $S_p = 15.942$ MeV. In order to determine branching ratios, decays via all available channels must be considered. This includes γ decay which, while suppressed at high excitations, must be considered near and below the n-decay threshold. This is because α decay is prohibited by angular momentum selection rules for low-lying unnatural parity states, due to the first non-0^+ state in the ^{14}C daughter nucleus lying at 6.094 MeV with $J^\pi = 1^-$ [25].

In order to distinguish between these decay channels, a kinematic technique known as a Catania plot (also known as a Romano plot) [16,17,19,26] was employed. A Catania plot is shown in Fig. 2, demonstrating how α- and n-decay events can be separated from one another. For the decay of an ^{18}O* nucleus, excited to an energy, E_x, into particles A and B, the total Q value is given by

$$Q_3 = E_A + E_B + E_p + E_x - E_{\text{beam}}, \tag{2}$$

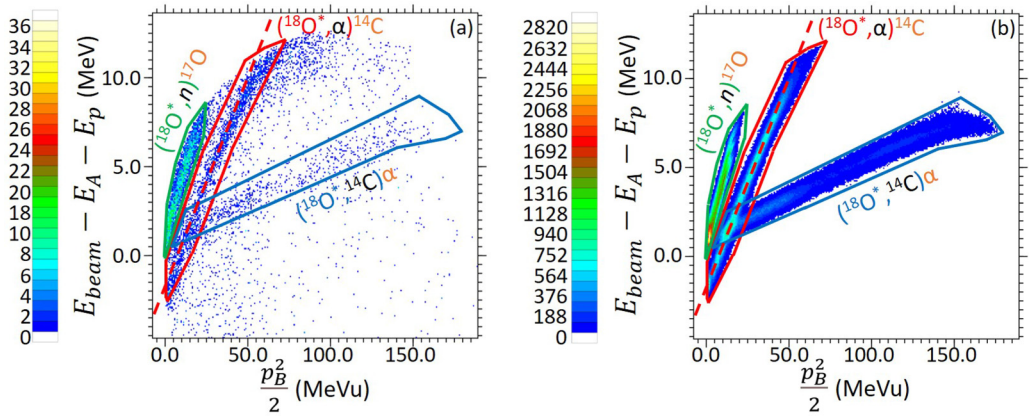

FIG. 2. Catania plots generated for decay products measured in the DSSD array for states in the 10.5 MeV region, assuming a detected ^{14}C from a (^{18}O*, α) decay, for real data (a) and simulated data (b). The different loci, identified via the Monte Carlo simulations, are labeled. Decay products shown outside of the brackets refer to the species detected in the DSSD array. The dashed line, upon which the detected ^{14}C locus lies, represents a gradient of 1/4 and an intercept -2.173, corresponding to the inverse of the mass of the undetected particle and $-Q$ of the total reaction respectively.

where E_A, E_B, E_p, and E_{beam} represent the kinetic energies of particles A, B, the recoil p detected in the Q3D and the beam, respectively. If particle A is then detected in the DSSD array, the measured energy and position can be used to calculate the momentum of A along each axis. The momenta of all particles other than B are hence known and B can be easily reconstructed via conservation of momentum, through

$$\vec{p}_B = \vec{p}_{\text{beam}} - \vec{p}_p - \vec{p}_A. \tag{3}$$

By rearranging Eq. (2) and substituting $E_B = \frac{p_B^2}{2m_B}$, the relationship

$$E_{\text{beam}} - E_p - E_A = \frac{1}{m_B} \times \frac{p_B^2}{2} - Q_3 + E_x, \tag{4}$$

is obtained. By plotting the quantity $E_{\text{beam}} - E_p - E_A$ against $\frac{p_B^2}{2}$ [obtained from Eq. (3)], a linear locus of gradient $1/m_B$ and intercept $-Q_3 + E_x$ was obtained for events in which the correct assumption about the detected mass, m_A, was made. Events which corresponded to different decays lie in other regions, which could be confirmed via Monte Carlo simulation. The corresponding line is shown in Fig. 2, as well other loci from an incorrect mass assumption, for events in the 10.5 MeV excitation region assuming the decay of ^{18}O* into $\alpha + {}^{14}$C.

B. Monte Carlo simulation

The in-house Monte Carlo code, RESOLUTION8.1 [19,27,28], was used to generate events for each observed excited state, simulating all available decay paths. Individual decay paths for each state were simulated using 10^7 events in order to determine the expected geometry efficiency of the DSSD array while limiting the associated statistical error. Events were simulated in which a recoil proton was incident in the solid angle corresponding to the angular acceptance of the Q3D, with decays from ^{18}O uniformly distributed in the center-of-mass frame. As a result, the fraction of decays detected by the DSSD array were determined through these Monte Carlo simulations. The simulations were also used to determine the fraction of individual channel events in overlapping loci of the Catania plots, using the method detailed in Ref. [19].

III. RESULTS

States were fitted across the observed excitation regions (see Fig. 3) with an average resolution of 65 keV across the focal-plane detector, originating from energy loss variations of the beam and recoil proton in the target. This resolution was determined by observation and subsequent fitting of the ground state and first excited state of ^{18}O. Widths (Γ_{tot}) were determined, assuming the measured full width at half-maximum (FWHM) consisted of a convolution of experimental resolution and the resonance function. The branching ratios for states were determined by normalizing across all of the observed decay channels, allowing for a measurement of $\Gamma_\alpha/\Gamma_{\text{tot}}$ for potential cluster states. Values of θ_α^2 were calculated assuming a channel radius for Eq. (1) of 5.6 fm and the relevant spin-parity as assigned by the proposed bands in Ref. [10]. The barrier penetrability of α particles decaying from each state was calculated using the measured excitation energy and the spins assigned from the proposed cluster bands, assuming a spherical geometry. This value ranged from 0.02 to 0.53, with the notable exception of the low-lying $J^\pi = 4^+$ state at 7.117 MeV, which had a calculated barrier penetrability of $5.2(1) \times 10^{-7}$. Uncertainties on these values were determined by varying the excitation energy by $\pm\sigma$. Typically, a value of $\theta_\alpha^2 \geqslant 0.1$ is considered to indicate clustering.

The background for fitted states, shown by dashed lines in Fig. 3, represents the different n phase space distributions: the two-body ^{17}O, n distribution between 8.045 MeV and 12.188 MeV, and the combination of the two-body and three-body ^{16}O, $2n$ distributions above 12.188 MeV. Below S_n, a constant background was fitted. The functional form of the background was extracted from Ref. [10] and scaled to match the spectra obtained - this was done for all decay channel spectra. The chosen scaling of the background results in a non-negligible

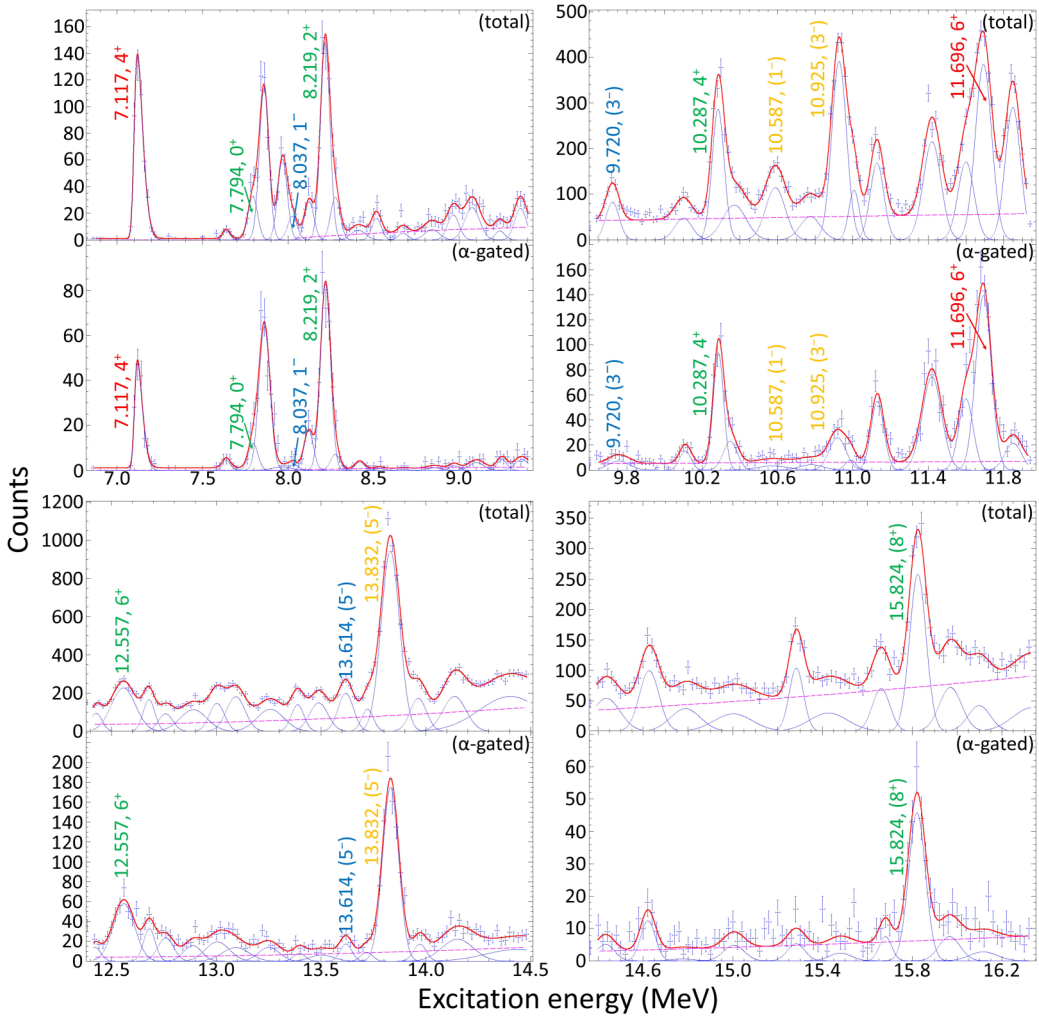

FIG. 3. The excitation regions investigated. Each region is shown in two panels with the Q3D-only spectrum (singles data only), labeled (total), and Q3D events gated on α-decay events, measured in the DSSD array, below. States labeled are the observed states that were proposed in Ref. [10] to be members of rotational bands (with tentative spin-parities shown in parentheses), with coloring as follows: red, $K^\pi = 0_2^+$; blue, $K^\pi = 0_2^-$; green, $K^\pi = 0_4^+$; orange, $K^\pi = 0_4^-$. See text and Table I for details.

systematic shift in measured branching ratios for wide states in the n-decay channel, where the background was expected and seen to be largest, resulting in a larger relative uncertainty than for other states. Figure 4 shows the efficiency-corrected backgrounds for each region, for the α- and n-decay channels, demonstrating very similar functional forms to the ungated Q3D singles profile. This is due to the change in detection efficiency over a given excitation region being negligible when compared with the experimental uncertainty.

Previous results for some of the states in the proposed rotational bands are presented here for comparison, notably the work of Avila *et al.* [6], and Yang *et al.* [7]. Avila *et al.* populated states in ^{18}O from 8.0 MeV to 15.0 MeV using the thick target inverse kinematics (TTIK) technique through ^{14}C$+\alpha$ elastic scattering, investigating $\Gamma_\alpha/\Gamma_{\rm tot}$ via resonant scattering and an R-matrix approach. Yang *et al.* [7] populated states via the ^{9}Be(^{13}C, ^{18}O)α reaction and measured lower limits for branching ratios of several states ranging from 10.3 MeV to 15.9 MeV. In addition, comparisons to results from Johnson *et al.* [9] which investigated states from 8.0 MeV to 11.0 MeV and Goldberg *et al.* [8] which investigated states from 9.0 MeV to 21.3 MeV, both utilizing ^{14}C$+\alpha$ elastic scattering via the TTIK method. The results and literature values are summarized in Table I, while the states that were found to display cluster structure are highlighted in Fig. 5.

A. The proposed $K^\pi = 0_2^+$ band

The states observed in the potential $K^\pi = 0_2^+$ band were the 4^+ 7.117 MeV and the 6^+ 11.696 MeV states. Due to the 7.117 MeV state lying below the neutron threshold, γ decay had to be taken into account using the method detailed in Ref. [17]. The value of $\Gamma_\alpha/\Gamma_{\rm tot}$ obtained was 0.49(2), representing the first-such measurement for this state. Using this value gave $\theta_\alpha^2 < 0.014$ when calculated using the upper limit of $\Gamma_{\rm tot}$ of < 17 fs (3.9×10^{-17} eV) [29,30], as due to the resolution of the Q3D, the fitting performed was not sensitive to the width of this state. It is therefore concluded that the 4^+ state is not a member of a cluster band, limited by the narrow $\Gamma_{\rm tot}$. It should, however, be noted that the value of $\Gamma_{\rm tot}$ was

TABLE I. A table summarizing the results obtained for states in the potential bands, compared with literature values. Errors shown in the table represent statistical errors and, where relevant, the error on geometric efficiency.

J^π (lit.) (from rot. bands)	E_{level} (MeV)	Γ_{tot} (keV)	$\Gamma_\alpha/\Gamma_{\text{tot}}$	Barrier penet.	θ_α^2	E_{level} (lit.)[a] (MeV)	Γ_{tot} (lit.)[a] (keV)	$\Gamma_\alpha/\Gamma_{\text{tot}}$(lit.)[b]
				$K^\pi = 0_2^+$				
4^+	7.117(2)	<16	0.49(2)	$5.2(1)\times10^{-7}$	<0.01[c]	7115(5)	<0.0004[d]	—
6^+	11.696(1)	74(3)	0.73(6)	0.02120(2)	0.4	11702(6)	19(7)	0.52(6), >0.89(3)
				$K^\pi = 0_2^-$				
1^-	8.037(5)	<33	0.34(9)	0.0528(7)	<0.004[c]	8.035(5)	<2.5[e]	1
(3^-)	9.720(5)	<20	0.26(7)	0.1301(6)	<0.007	9.715(5)	15(4)	0.27(5)
(5^-)	13.614(3)	<23	0.15(3)	0.2350(2)	<0.002	13.624(6)	22(7)	>0.07(1)
				$K^\pi = 0_4^+$				
0^+	7.794(2)	<16	>0.63(5)	0.0422(3)	0.07[f]	7.796(5)	<10	—
2^+	8.219(1)	<13	0.88(2)	0.03258(9)	0.01[c]	8.216(5)	1.9(2)[g]	0.89(11)
4^+	10.287(1)	40(6)	0.60(4)	0.07951(8)	0.05	10.293(6)	23(8)	0.66(11)
6^+	12.557(2)	107(8)	0.63(5)	0.04726(8)	0.2	12.557(7)	22(8)	0.7(2), >0.79(3)
(8^+)	15.824(2)	55(7)	α_0: 0.38(10)	0.02882(3)	0.08[h]	15.810(10)	20(8)	>0.57(2)
				$K^\pi = 0_4^-$				
(1^-)	10.587(3)	96(10)	<0.12	0.5268(4)	<0.003	10.59(1)	70(16)	—
(3^-)	10.919(4)	30(20)	0.18(4)	0.2940(5)	0.003	10.92(1)	30(9)	—
(5^-)	13.832(1)	73(3)	0.38(3)	0.2528(1)	0.01	13.82(2)	27(8)	0.12(5), >0.32(2)

[a]Values from Ref. [10], except in certain cases denoted by extra footnotes.
[b]See text for details.
[c]Value of θ_α^2 calculated using literature width, due to limits of experimental resolution.
[d]Width taken from Ref. [29], calculated using data from Ref. [30].
[e]Width from Ref. [31].
[f]Value of θ_α^2 presented without limit, due to conflicting limits on Γ_{tot} and $\Gamma_\alpha/\Gamma_{\text{tot}}$.
[g]Width taken from Ref. [6].
[h]Calculated using α_0 value.

not established from direct measurement, and if the width of the state were determined accurately and found to be an order of magnitude larger than that presented in Refs. [29,30], the value of θ_α^2 would increase to above 0.1. The 11.696 MeV

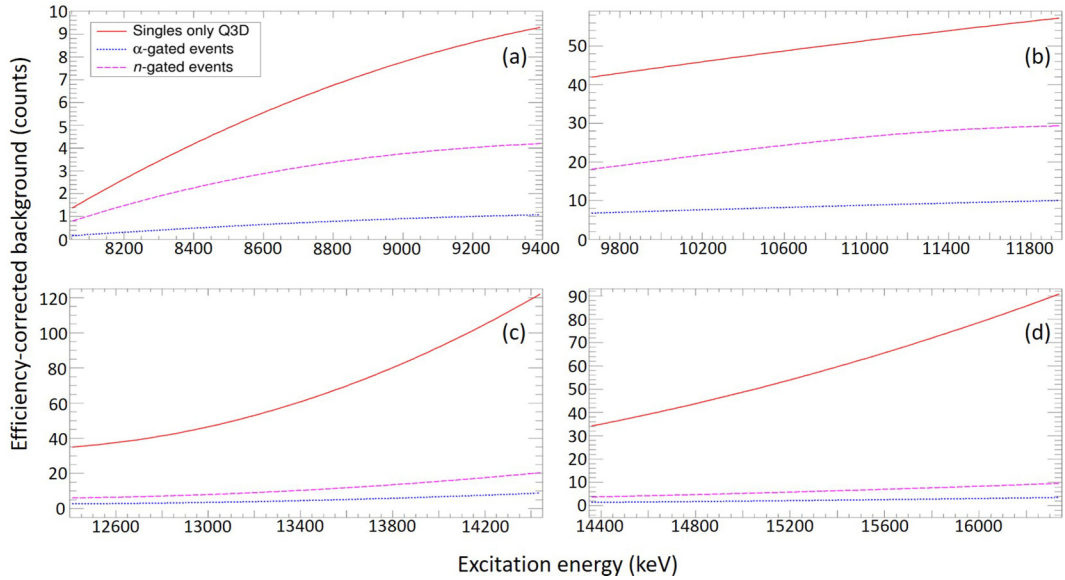

FIG. 4. Efficiency-corrected background profiles for the (a) 7800 keV, (b) 10500 keV, (c) 13200 keV and (d) 15100 keV regions, calculated as the product of the scaled background for each spectrum multiplied by the geometric efficiency profile across the excitation region. The red solid line, dashed magenta line and dotted blue line represent the background profile from the Q3D singles only, α-gated and n-gated events respectively. This demonstrates that the functional form is unchanged by efficiency correction due to uncertainties being larger than efficiency effects.

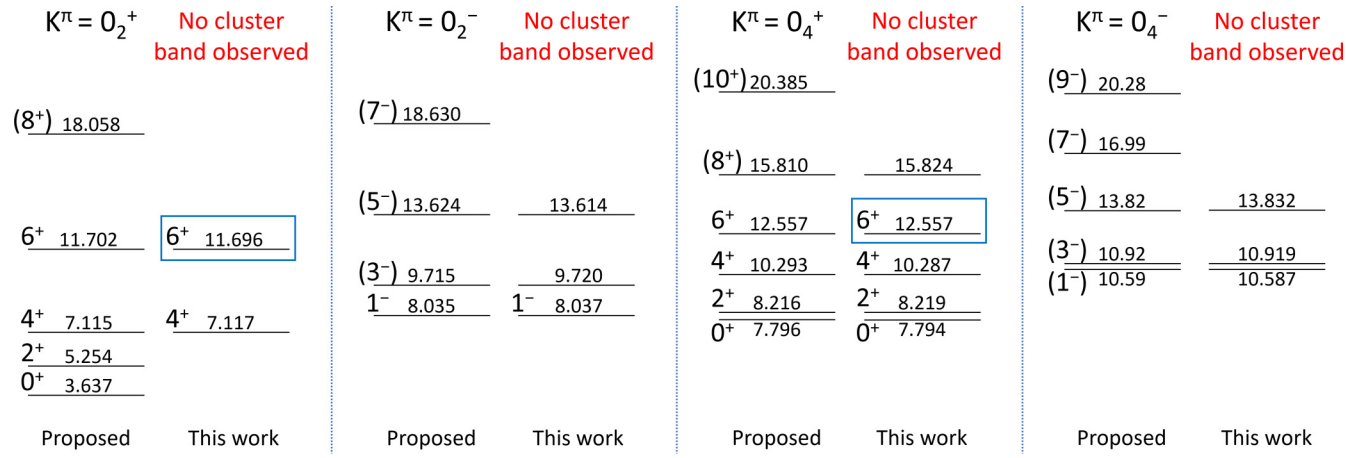

FIG. 5. A depiction of the states proposed to exist in the cluster bands, with observed excitation energies (given in MeV) from Ref. [10], compared to the results from this work. States determined to display cluster structure are shown in boxes.

6^+ state was measured to have $\Gamma_\alpha/\Gamma_{\rm tot} = 0.73(6)$, a value that lies between that measured by Avila *et al.* [6] via resonant scattering of 0.52(6) and the lower limit determined by Yang *et al.* [7] of >0.89(3). The mean of these two values gives $\Gamma_\alpha/\Gamma_{\rm tot} = 0.82(15)$, which lies within 1σ of the value from the current work. Using $\Gamma_{\rm tot} = 74(3)$ keV from the fit of the excitation spectrum, a value of $\theta_\alpha^2 = 0.39$ is obtained, suggesting that this state does indeed possess a cluster structure.

B. The proposed $K^\pi = 0_2^-$ band

The observed states from the proposed $K^\pi = 0_2^-$ band were the 1^- 8.037 MeV, (3^-) 9.720 MeV, and (5^-) 13.614 MeV resonances. For 8.037 MeV, the value of $\Gamma_\alpha/\Gamma_{\rm tot}$ measured was 0.34(9). While this is not in agreement with the result from Avila *et al.* [6], which measured 100% of the strength of this resonance belonging to the α branch, this current measurement is sensitive to the γ branch, to which the majority of decays for this state belong. Using the upper limit of $\Gamma_{\rm tot} < 2.5$ keV [31], a value of $\theta_\alpha^2 < 0.004$ is obtained, which suggests that this state does not represent a clustered band head. The 9.720 MeV state appears to be a combination of two closely-separated states, as the centroid of the resonance changes from 9.711(4) MeV when gated by n-decay events to 9.760(12) MeV when gated by α-decay events. The existence of a further, weakly populated majority α-decaying state is in good agreement with previous measurements [6,8,9] in this region. The value $\Gamma_\alpha/\Gamma_{\rm tot} = 0.26(7)$ for this combined part is consistent with the value of 0.27(5) measured by Goldberg *et al.* [8], and produces $\theta_\alpha^2 < 0.007$ from the upper limit $\Gamma_{\rm tot} < 20$ keV. The 13.614 MeV state is measured to have $\Gamma_\alpha/\Gamma_{\rm tot} = 0.15(3)$ here, in agreement with the upper limit measurement of Ref. [7], $\Gamma_\alpha/\Gamma_{\rm tot} > 0.07(1)$. Together with the measured width, <23 keV, a value of $\theta_\alpha^2 < 0.002$ is obtained. It can clearly be seen that none of these states display cluster structure, and thus the cluster band does not exist.

C. The proposed $K^\pi = 0_4^+$ band

The band head of this proposed band lies at 7.794 MeV and has $J^\pi = 0^+$, determined by angular distributions [10]. There is difficulty in resolving this state, as there also exists a 2^- state at 7.770 MeV which lies well within the experimental resolution of the 0^+ level. By presenting both states convoluted, the value of $\Gamma_\alpha/\Gamma_{\rm tot}$ represents a lower limit for the 7.794 MeV state due to the inability of the 7.770 MeV state to α decay. Taking $\Gamma_\alpha/\Gamma_{\rm tot} = 0.63(5)$ and, using the measured width of < 16 keV, a value of $\theta_\alpha^2 = 0.07$ is obtained—this could increase depending on the true α branch of the state, but it is likely this state does not display cluster structure as the true width of the state may be much lower, while the corresponding $\Gamma_\alpha/\Gamma_{\rm tot}$ cannot be >1. The 8.219 MeV 2^+ state lies above the n-decay threshold, and decays not due to the α branch, from either n decay or γ decay, are indistinguishable due to overlapping loci on Catania plot, as well as the extremely similar geometric efficiencies of the n and γ branches just above the n threshold. As the geometric efficiencies are so similar, assuming all of these non-α events arise from n decay has no effect on the measured value of the α branch. The effect on the n-branch decreases as excitation energy increases and the γ branch is suppressed. The value of $\Gamma_\alpha/\Gamma_{\rm tot} = 0.88(2)$ measured in the current work agrees with that measured in Ref. [6] of 0.89(11) to within 1σ, while reducing the uncertainty by an order of magnitude. Together with the measured width from Ref. [6], a value of $\theta_\alpha^2 = 0.01$ is obtained, suggesting that this state does not display cluster structure. The 10.287 MeV 4^+ state is well populated, with $\Gamma_\alpha/\Gamma_{\rm tot} = 0.60(4)$. This value is consistent with previous measurements, 0.66(0.11) [6] and >0.37(3) [7]. The width measured in this work is 40(6) keV, resulting in $\theta_\alpha^2 = 0.05$. The 6^+ state lies at 12.557 MeV, with a measured width of 107(8) keV. The measured value of $\Gamma_\alpha/\Gamma_{\rm tot} = 0.63(5)$ is consistent with the value obtained by Ref. [6] of 0.7(2), but lower than that measured by Ref. [7] of >0.79(3). The large discrepancy in width with literature values may suggest a convolution of states in this region in the current work, unable to be clearly separated due to the experimental resolution. A state at 15.824 MeV, predicted to have $J^\pi = 8^+$ based on being a member of the proposed band, was observed in the current work. The measured value of $\Gamma_{\alpha 0}/\Gamma_{\rm tot} = 0.38(10)$ is within two standard deviations of the result measured in Ref. [7]

of >0.57(2). However, there is also a large α branch that passes through an excited state in ^{14}C (7.012 MeV, $J^\pi = 2^+$), suggested, through comparison to Monte Carlo simulation and the requirement that the excited level be natural parity due to selection rules made evident by the existence of decays to the ground state of ^{14}C, to be $\Gamma_{\alpha 5}/\Gamma_{\rm tot} = 0.51(10)$. However, a notable centroid shift occurs [≈20 keV, to 15.841(4) MeV] when looking at events passing though the excited level of ^{14}C. It is therefore possible that this region contains a convolution of a natural and unnatural parity state which have a separation much less than the experimental resolution of this work, and these decays pass through the 6.903 MeV $J^\pi = 0^-$ state, the lowest-lying determined unnatural parity state in ^{14}C, as the comparison to Monte Carlo data is not sensitive to a 100 keV shift in the excitation energy of the daughter nucleus. This state is the only state to suggest decay through an excited level in the daughter ^{14}C in the experimental data.

D. The proposed $K^\pi = 0_4^-$ band

There are three observed states in this proposed negative-parity rotational band, lying at measured energies of 10.587(3) MeV (1^-), 10.919(4) MeV (3^-), and 13.832(1) MeV (5^-). These spin-parities are all tentative, arising in-part from rotational fitting [10].

The 10.587 MeV state was observed to have $\Gamma_\alpha/\Gamma_{\rm tot} < 0.12$, much lower than expected for a cluster state with a low spin. This represents the first measurement of this value by any method, and using the measured width of 96(10) keV gives $\theta_\alpha^2 < 0.003$, indicating a lack of cluster structure for this state.

The 10.919 MeV state was strongly-populated, in convolution with a weakly populated state at 10.985(6) MeV. The current work measures $\Gamma_\alpha/\Gamma_{\rm tot} = 0.18(4)$ for the 10.919 MeV state, again representing a first measurement of this value. Due to the convolution of the peaks, there was a reasonable uncertainty on the value of the width, measured here to be 30(20) keV. This gives $\theta_\alpha^2 = 0.003$, again indicating that this state does not belong to a cluster band.

The highest energy state observed in this proposed rotational band was the 5^- 13.832 MeV state. This state was well populated, convoluted with two smaller states (one either side) of energies 13727(5) keV and 13965(1) keV; as the centroids of these states were at least 100 keV away from each other, resolving them was possible. The value of $\Gamma_\alpha/\Gamma_{\rm tot}$ was measured to be 0.38(3), in agreement with the value of >0.32(2) from Ref. [7]. A value of 0.12(5) is reported in Ref. [6], measured through resonant scattering, though this discrepancy may be due to the high level-density in this region. The width of this state was determined to be 73(3) keV, which results in $\theta_\alpha^2 = 0.01$, suggesting an absence of α clustering in the structure of this excitation.

E. The proposed $K^\pi = 1^-$ band

The proposed $K^\pi = 1^-$ band had potential members within the observed excitation regions. One state of interest is at 11.127(2) MeV, suggested to be a 4^- as a member of this band. The value $\Gamma_{\alpha 0}/\Gamma_{\rm tot} = 0.68(6)$ was extracted, disproving this state assignment as unnatural parity α decays are disallowed to the ground state of ^{14}C, and this excitation energy is too low to populate the first excited state. This result is in good agreement with the value from Ref. [7] of >0.65(3) and within two standard deviations of 0.8, presented without error from Ref. [8].

IV. DISCUSSION AND SUMMARY

No members of either negative-parity band are seen to display cluster structure in the current work, with all values of θ_α^2 determined to be 0.01 or below. This has implications for both potential positive-parity bands, regardless of other results, as theory predicts that the cluster bands with structures $^{14}\mathrm{C} \otimes \alpha$ and $^{12}\mathrm{C} \otimes 2n \otimes \alpha$ should have negative-parity bands due to their intrinsic reflection asymmetry.

The measurement of the $J^\pi = 4^+$ state of the $K^\pi = 0_2^+$ band in the current work suggests that, if the band were to exist, this 7.117 MeV state cannot belong to it, as $\theta_\alpha^2 < 0.01$. It should be noted that this is highly dependent on the width of the state, which the current work is insensitive to due to the experimental resolution. However, any measured width of this state would need to be an order of magnitude larger to be consistent with cluster structure. The $J^\pi = 6^+$ member at 11.696 MeV appears to display cluster structure, as previously suggested by measurements from Ref. [7].

The $K^\pi = 0_4^+$ band does not display consistent cluster structure across the suggested members, with the $J^\pi = 2^+$ 8.219 MeV state and the $J^\pi = 4^+$ 10.287 MeV state displaying $\theta_\alpha^2 = 0.01$ and $\theta_\alpha^2 = 0.05$, respectively. The $J^\pi = 6^+$ does seem to exhibit cluster structure, in part due to the large width measured in this work. The possibility that a high level density in this area causes issues resolving individual states should be considered, although this state has been measured to show cluster structure previously [6,7] with $J^\pi = 6^+$. Conclusions about the potential band head at 7.794 MeV are tentative due to difficulty in resolving it; however, it seems unlikely that this state is clustered, as the width of the state is likely to be substantially lower than the upper limit determined in this work due to the state being below the n-decay threshold and only 1.5 MeV above the α-decay threshold. Hence, the calculated value of θ_α^2 would decrease. It therefore seems unlikely that this band exists, as at least two of the members are seen to not exhibit cluster structure.

The only states that are seen to display significant cluster structure, the $J^\pi = 6^+$ 11.696 MeV and the $J^\pi = 6^+$ 12.557 MeV states, both having the same value of J^π, and due to the lack of band structure observed in this work, suggests the potential for fragmented clustering in ^{18}O, a phenomenon more commonly observed in midmass nuclei [32]. This has been previously suggested by measurements by Avila *et al.* [6].

In conclusion, energy levels in ^{18}O were observed from 7.1 MeV to 16.3 MeV through utilization of the $^{12}\mathrm{C}(^7\mathrm{Li}, p)\,^{18}\mathrm{O}^*$ reaction, using the Q3D magnetic spectrograph to detect recoil protons and the Birmingham large-angular-coverage DSSD array to record ^{18}O break-up

particles in coincidence. An experimental technique, sensitive to almost all branches, excluding β decay and electron capture, but including the population of excited levels in daughter nuclei, was employed to determine the associated α_0-branching ratios via high-resolution reconstruction of the decay channels. These branching ratios were used to calculate the tendency towards clustering of each state, using the measured excitation energies and widths of the states to determine θ_α^2. No evidence of the proposed bands was observed, with each proposed band containing members which clearly showed no cluster structure.

ACKNOWLEDGMENTS

The authors would like to thank A. Bergmaier for his help loaning equipment during the setup of the experiment, as well as the operators of the Van de Graaff Tandem accelerator at the Maier-Leibnitz Laboratory in Munich for providing and maintaining the ^{7}Li beam. This work was funded by the UK Science and Technology Facilities Council (STFC) under Grant Nos. ST/L005751/1 and ST/P004199/1, and by the European Union's Horizon 2020 research and innovation programme under the Marie Skłodowska-Curie Grant Agreement No. 65F9744.

[1] M. Freer, Scholarpedia **5**, 9652 (2010), revision no. 137031.
[2] B. R. Fulton, Contemp. Phys. **40**, 299 (1999).
[3] W. von Oertzen, Eur. Phys. J. A **11**, 403 (2001).
[4] J. Hiura, Y. Abe, S. Saitł, and O. Endł, Progr. Theor. Phys. **42**, 555 (1969).
[5] M. Freer, H. Horiuchi, Y. Kanada-En'yo, D. Lee, and Ulf.-G. Meißner, Rev. Mod. Phys. **90**, 035004 (2018).
[6] M. L. Avila, G. V. Rogachev, V. Z. Goldberg, E. D. Johnson, K. W. Kemper, Y. M. Tchuvil'sky, and A. S. Volya, Phys. Rev. C **90**, 024327 (2014).
[7] B. Yang, Y. L. Ye, J. Feng, C. J. Lin, H. M. Jia, Z. H. Li, J. L. Lou, Q. T. Li, Y. C. Ge, X. F. Yang, H. Hua, J. Li, H. L. Zang, Q. Liu, W. Jiang, C. G. Li, Y. Liu, Z. Q. Chen, H. Y. Wu, C. G. Wang, W. Liu, X. Wang, J. J. Li, D. W. Luo, Y. Jiang, S. W. Bai, J. Y. Xu, N. R. Ma, L. J. Sun, D. X. Wang, Z. H. Yang, and J. Chen, Phys. Rev. C **99**, 064315 (2019).
[8] V. Goldberg, K.-M. Källman, T. Lönnroth, P. Manngård, and B. Skorodumov, Phys. At. Nucl. **68**, 1079 (2005).
[9] E. D. Johnson, G. V. Rogachev, V. Z. Goldberg, S. Brown, D. Robson, A. M. Crisp, P. D. Cottle, C. Fu, J. Giles, B. W. Green, K. W. Kemper, K. Lee, B. T. Roeder, and R. E. Tribble, Eur. Phys. J. A **42**, 135 (2009).
[10] W. von Oertzen, T. Dorsch, H. G. Bohlen, R. Krücken, T. Faestermann, R. Hertenberger, Tz. Kokalova, M. Mahgoub, M. Milin, C. Wheldon, and H.-F. Wirth, Eur. Phys. J. A **43**, 17 (2009).
[11] K. P. Artemov, V. Z. Goldberg, M. S. Golovkov, B. G. Novatskij, I. P. Petrov, V. P. Rudakov, I. N. Serikov, and V. A. Timofeev, Yad. Fiz. **37**, 1351 (1983).
[12] G. Morgan, D. Tilley, G. Mitchell, R. Hilko, and N. Roberson, Nucl. Phys. A **148**, 480 (1970).
[13] H. T. Fortune, Phys. Rev. C **18**, 1053 (1978).
[14] N. Curtis, D. D. Caussyn, C. Chandler, M. W. Cooper, N. R. Fletcher, R. W. Laird, and J. Pavan, Phys. Rev. C **66**, 024315 (2002).
[15] I. J. Thompson and F. M. Nunes, *Nuclear Reactions for Astrophysics* (Cambridge University Press, Cambridge, 2009), p. 303.
[16] C. Wheldon, N. I. Ashwood, M. Barr, N. Curtis, M. Freer, T. Kokalova, J. D. Malcolm, S. J. Spencer, V. A. Ziman, T. Faestermann, R. Krücken, H.-F. Wirth, R. Hertenberger, R. Lutter, and A. Bergmaier, Phys. Rev. C **83**, 064324 (2011).
[17] S. Pirrie, Tz. Kokalova, C. Wheldon, S. Bailey, J. Bishop, N. Curtis, R. Smith, D. Torresi, A. Turner, R. Hertenberger *et al.*, in *Proceedings of the 4th International Workshop on "State of the art in Nuclear Cluster Physics" (SOTANCP4)*, edited by M. Barbui, C. M. Folden, V. Z. Goldberg, and G. V. Rogachev, AIP Conf. Proc. No. 2038 (AIP, New York, 2018), p. 020037.
[18] S. Pirrie, C. Wheldon, Tz. Kokalova, J. Bishop, R. Hertenberger, H.-F. Wirth, S. Bailey, N. Curtis, D. Dell'Aquila, Th. Faestermann *et al.*, J. Phys.: Conf. Ser. (27th International Nuclear Physics Conference) (to be published).
[19] S. Pirrie, C. Wheldon, T. Kokalova, J. Bishop, R. Hertenberger, H.-F. Wirth, S. Bailey, N. Curtis, D. Dell'Aquila, T. Faestermann, D. Mengoni, R. Smith, D. Torresi, and A. Turner, SciPost Phys. Proc. **3**, 009 (2020).
[20] C. Wiedner, M. Goldschmidt, D. Rieck, H. Enge, and S. Kowalski, Nucl. Instrum. Methods **105**, 205 (1972).
[21] M. Löffler, H. Scheerer, and H. Vonach, Nucl. Instrum. Methods **111**, 1 (1973).
[22] H.-F. Wirth, Ph.D. thesis, Technische Universität München, München, 2001.
[23] H. Scheerer, H. Vonach, M. Löffler, A. Decken, M. Goldschmidt, C. Wiedner, and H. Enge, Nucl. Instrum. Methods **136**, 213 (1976).
[24] W1 DSSDs made by Micron Semiconductor Ltd., http://www.micronsemiconductor.co.uk/strip-detectors-double-sided/ (2015), accessed 2019-10-15.
[25] R. B. Firestone, *Table of Isotopes*, 8th ed. (Wiley VCH, Weinheim, Germany, 1996).
[26] E. Costanzo, M. Lattuada, S. Romano, D. Vinciguerra, and M. Zadro, Nucl. Instrum. Methods **295**, 373 (1990).
[27] N. Curtis, Ph.D. thesis, University of Birmingham, UK, 1995.
[28] R. Smith, Ph.D. thesis, University of Birmingham, UK, 2017.
[29] M. Gai, M. Ruscev, D. A. Bromley, and J. W. Olness, Phys. Rev. C **43**, 2127 (1991).
[30] M. Hass, Z. Shkedi, D. Start, Y. Wolfson, and Y. Horowitz, Nucl. Phys. A **220**, 217 (1974).
[31] D. Tilley, H. Weller, C. Cheves, and R. Chasteler, Nucl. Phys. A **595**, 1 (1995).
[32] S. Bailey, T. Kokalova, M. Freer, C. Wheldon, R. Smith, J. Walshe, N. Curtis, N. Soić, L. Prepolec, V. Tokić, F. M. Marqués, L. Achouri, F. Delaunay, Q. Deshayes, M. Parlog, B. Fernández-Dominguez, B. Jacquot, and A. Soylu, Phys. Rev. C **100**, 051302(R) (2019).